An *In Situ* X-ray Absorption Spectroscopy Study of InSb Electrodes in Lithium Batteries

In the search for superior negative electrodes for Li-based batteries, *in situ* EXAFS studies have been performed on batteries containing InSb electrodes. The investigations provide crucial information on the sequence for the electrochemical lithiation of InSb as a function of charging voltage.
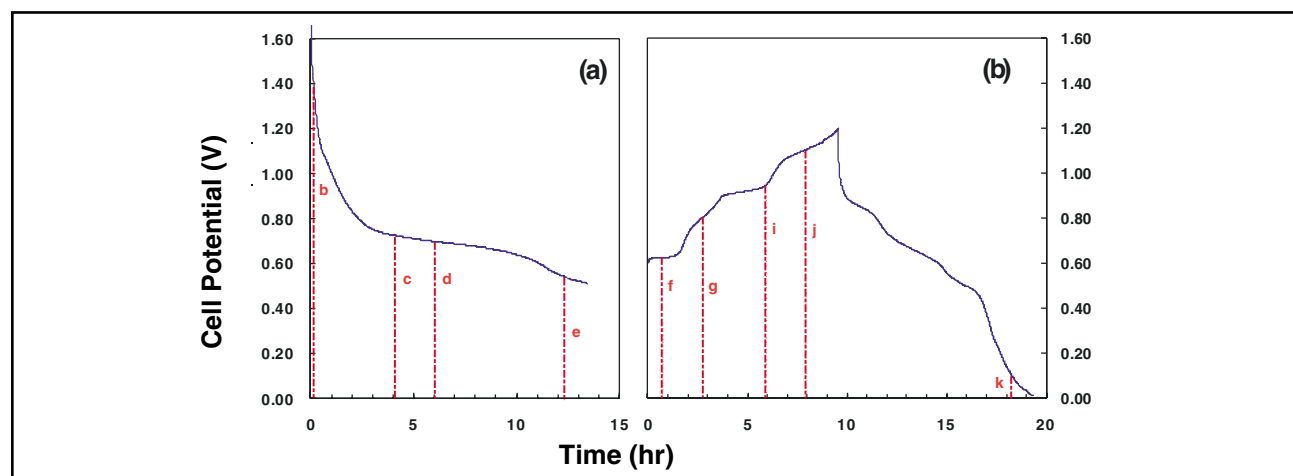

FIG. 1. Galvanostatic cell potential vs time curves for cell A (a: discharging of a freshly prepared cell at a constant current density of 0.3 mA/cm^2) and cell B (b: charging and subsequent discharging of a precycled cell at constant current densities of 0.4 mA/cm^2 and 0.5 mA/cm^2, respectively). The voltages corresponding to the EXAFS spectra shown in Fig. 2 are marked with dotted lines.

Rechargeable lithium-ion batteries are becoming increasingly prominent as power sources for electronic consumer products, such as cellular phones, camcorders, laptop computers, and the like. In light of their impressive performance in electronic devices, their high energy and capacity per unit weight, and their rechargability, lithium-ion batteries are also becoming leading candidates for powering electric and hybrid-electric vehicles. State-of-the-art lithium-ion batteries contain 4-V cells composed of lithiated graphite (LiC$_6$) negative electrodes coupled to lithium/transition metal–oxide positive electrodes via an organic electrolyte. These batteries are fraught with inherent safety and reliability issues and require sophisticated electronic circuitry to protect individual cells from being overcharged. Because many of the safety issues are related to the negative electrode, a pressing need exists for an alternative material to graphite that will reduce the safety hazards, improve the performance, and increase the useful cycle life of lithium-ion batteries.

We have recently reported that intermetallic compounds such as Cu$_6$Sn$_5$, InSb, and Cu$_2$Sb exhibit promising structural and electrochemical properties when used as negative electrodes for lithium-ion batteries [1-5]. What is particularly attractive is that these materials do not exhibit the large volume expansion upon reaction with lithium found in other types of intermetallic electrodes. The aim of this study is to determine the changes in structure and composition of InSb electrodes by analysis of extended x-ray absorption fine structure (EXAFS) spectra obtained *in situ* during electrochemical cycling of coin-type cells that mimic commercially available batteries.
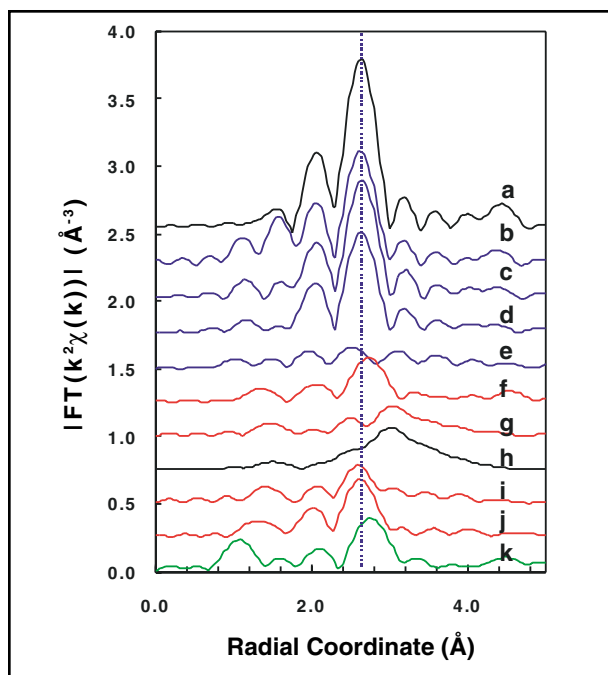
FIG. 2. Magnitude of the Fourier transform (FT) of the k^2-weighted In-edge EXAFS from a coin cell containing an InSb electrode as a function of applied potential (refer to Fig. 1 for comparison to the potential vs time diagram): (a) powdered single-crystal InSb; (b) cell A, 1.47 V; (c) cell A, 0.72 V; (d) cell A, 0.69 V; (e) cell A, 0.53 V; (f) cell B, 0.62 V; (g) cell B, 0.80 V; (h) In metal foil; (i) cell B, 0.94 V; (j) cell B, 1.10 V; and (k) cell B, 0.10 V. (Cell A, blue spectra; cell B charge cycle, red spectra; cell B discharge cycle, green spectrum; $\Delta k = 2.5 – 11.0$ Å^{-1}, $dk = 0.5$ Å^{-1}.)

The EXAFS measurements were performed on the insertion device beamline of the Materials Research Collaborative Access Team (MR-CAT) [6]. To achieve time resolution suitable for following the electrochemical reactions, EXAFS spectra were taken in a continuous scan mode. By increasing the measurement speed in this way, we could maintain a constant current in Li/InSb electrochemical cells for the duration of the experiments, rather than interrupt the current periodically to make long EXAFS measurements. This scan rate was fast enough to ensure that the potential did not change by more than 0.02 V over a complete scan, except in the steeply sloped regions of the potential versus time curve.

Plots of the electrochemical potential versus time of Li/InSb cells are shown in Fig. 1. Figure 1a represents the initial "conditioning" discharge reac-

tion of one cell (Cell A) to 0.5 V, in which some irreversible changes occur in the electrode. Figure 1b shows the first charge to 1.2 V and subsequent discharge to 0 V of a second cell (Cell B) after an offline conditioning discharge to 0.5 V. The magnitudes of the Fourier transform at selected cell potentials (indicated in Fig. 1) are shown in Fig. 2. During the conditioning discharge the structural changes as Li is first inserted into InSb are relatively minor, although a slight increase in the In-Sb distance, $R_{\text{In-Sb}}$, is detected (spectra b and c in Fig. 2).

Evidence of In extrusion during the conditioning cycle becomes visible at 0.70 ± 0.02 V and manifests itself as a slight decrease in the amplitude of the first-shell In-Sb peak ($N_{\text{In-Sb}}$) in the Fourier transform (spectrum d). The position of the In-Sb path is designated by the vertical dotted line in Fig. 2. Subsequently, $N_{\text{In-Sb}}$ decreases as In is extruded from the face-centered-cubic (fcc) Sb lattice to leave a structure closely resembling Li_3Sb, although the characteristic In metal scattering paths cannot be fitted reliably until the potential decreases below 0.62 V (spectrum e). Lithiation of the extruded In occurs at approximately 0.55 V to yield LiIn.

On charging Cell B from 0.5 to 1.2 V, LiIn first reverts to metallic In on the plateau at 0.62 V. At this potential, an analysis of the EXAFS data (spectrum f, Fig. 2) shows that the In distribution in the electrode is approximately 70% in LiIn, 20% in In metal, and 10% in a lithiated zinc-blende-type "composite" structure, represented generally as $Li_xIn_{1-y}Sb$, for which x and y can fall within the ranges $0 < x < 3$ and $0 < y < 1$. The dominant presence of In metal in the electrode at 0.80 V can be seen by comparing the EXAFS data collected at this voltage to the EXAFS data of a standard In metal foil. At 0.80 V, the In distribution is approximately 90% In metal and approximately 10% In within $Li_xIn_{1-y}Sb$. The EXAFS signal of the electrode at 0.94 V indicates that a zinc-blende-type structure with increasing In content is regenerated as lithium is extracted electrochemically. Near the top of charge, at 1.1 V, the amplitude of the nearest-neighbor In-Sb path is smaller than in the initial electrode, indicating that the displaced In has not been entirely
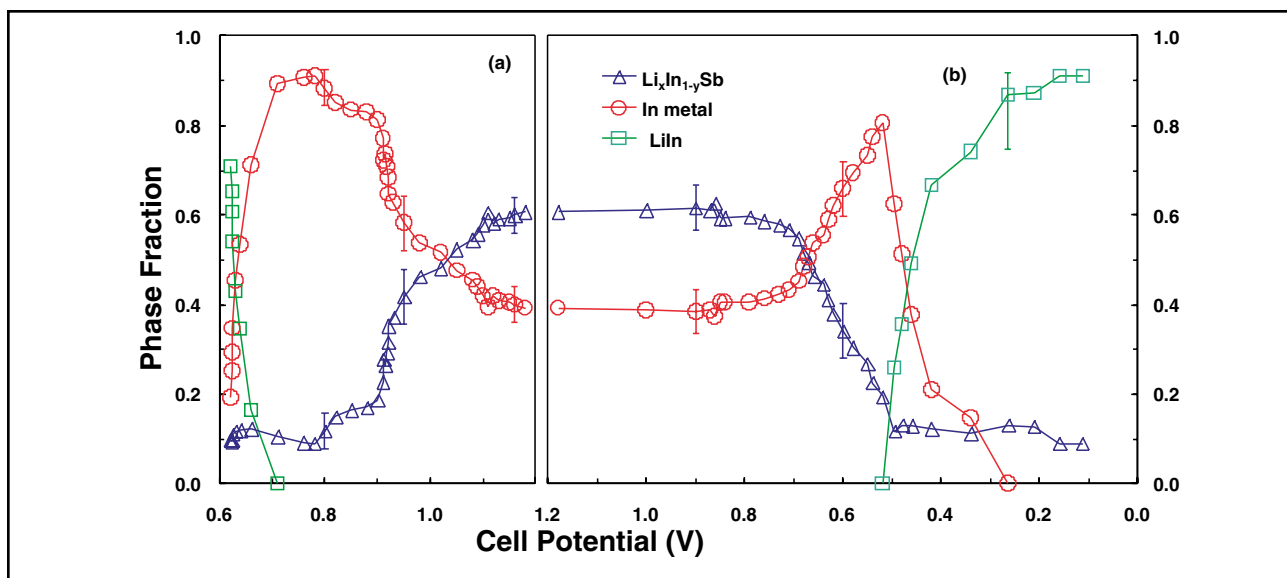
FIG. 3. Phase distribution of indium atoms as a function of cell potential upon (a) charging and (b) discharging: $Li_xIn_{1-y}Sb$ (triangles), metallic In (circles), and LiIn (squares). Error bars are shown for representative points.

reincorporated into the fcc Sb array. In fact, a quantitative analysis of the EXAFS data shows that as much as 40% of the In remains as the tetragonal, elemental phase outside the Sb framework.

On the subsequent discharge, Cell B was discharged from 1.2 V to 0 V (Fig. 1b). The voltage profile between 1.2 and 0.5 V confirms the reversibility of the processes that were described above for the charge reactions. The EXAFS spectrum obtained at 0.1 V, although not yet fully interpreted, is believed to correspond to structures in the Li_xIn system for $(1 \leq x \leq 4)$. Figure 3 summarizes the results of the quantitative analyses of the EXAFS data obtained during the charge and discharge of Cell B; in this figure, the phase fractions of In as In metal, LiIn, and $Li_xIn_{1-y}Sb$ are plotted as a function of the cell potential.

These *in situ* EXAFS data, therefore, provide valuable information about the complex reactions that occur when Li is inserted into, and In extruded from, a fixed fcc Sb array to yield metastable $Li_xIn_{1-y}Sb$ composite structures for $0 < x < 3$ and $0 < y < 1$. According to our analysis of the EXAFS data, the sequence for the electrochemical lithiation of the InSb to 0.5 V follows three main reactions:

I: δ Li + InSb → $Li_\delta InSb$
II: $(x-\delta)$ Li + $Li_\delta InSb$ → $Li_xIn_{1-y}Sb$ + y In
III: Li + In → LiIn
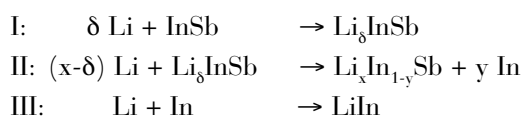
During reaction I, Li atoms partially occupy the interstitial sites of the InSb zinc-blende structure. During reaction II, Li insertion is accompanied by In extrusion, yielding $Li_xIn_{1-y}Sb$, in which $(x-\delta)$ Li atoms occupy either additional interstitial sites or the positions in the InSb zinc-blende framework left vacant by the extruded In atoms. The extent to which Li is inserted before In extrusion (δ) is not yet accurately known but is believed to be small. However, early In extrusion has not been detected in our EXAFS experiments, since we have found neither a reduced In-Sb coordination number nor the presence of metallic In above 0.72 V. In reaction III, lithiation of the extruded In occurs at approximately 0.55 V.

Li/InSb cells cycle well after one "conditioning" cycle when the discharge and charge reactions are limited to a voltage range over which the primary mechanisms are Li insertion and In extrusion (i.e., greater than 0.55 V). The good electrochemical reversibility of InSb electrodes is attributed to the existence of a stable fcc Sb framework that undergoes lattice parameter expansion of only 1.4% during the transformation of InSb to Li_3Sb. The fast mobility of In within the fcc Sb array during charge and discharge also plays an important role in the performance of these electrodes. Further research is currently being undertaken at Argonne National

Laboratory to exploit intermetallic electrode systems that operate by reversible lithium insertion/metal extrusion reactions in the hope of finding an alternative negative electrode to graphite for lithium-ion cells.

Principal publication: "An *In Situ* X-ray Absorption Spectroscopy Study of InSb Electrodes in Li Batteries," Electrochem. Commun. **3**, 244-251(2001).

REFERENCES
[1] A.J. Kropf, H. Tostmann, C.S. Johnson, J.T. Vaughey, and M.M. Thackeray, Electrochem. Comm. **3**, 244-251 (2001).

[2] K.D. Kepler, J.T. Vaughey, and M.M. Thackeray, Electrochem. and Solid State. Lett. **2**, 307 (1999).

[3] J.T. Vaughey, J.O. O'Hara, and M.M. Thackeray, Electrochem. and Solid State Lett. **3**, 13 (2000).

[4] C.S. Johnson, J.T. Vaughey, M.M. Thackeray, T. Sarakonsri, S.A. Hackney, L. Fransson, K. Edström, and J.O. Thomas, Electrochem. Comm. **2**, 595 (2000).

[5] L.M.L. Fransson, J.T. Vaughey, R. Benedek, L. Fransson, K. Edström, J.O. Thomas, and M.M. Thackeray, Electrochem. Comm. **3**, 317 (2001).

[6] C.U. Segre, N.E. Leyarovska, W.M. Lavender, P.W. Plag, A.S. King, A.J. Kropf, B.A. Bunker, K.M. Kemner, P. Dutta, R.S. Duran, and J. Kaduk, in Synchrotron Radiation Instrumentation: 11th U.S. National Conference, CP521, edited by P. Pianetta et al. (American Institute of Physics, New York, 2000), p. 419.

A. J. Kropf,[1] H. Tostmann,[2] C. S. Johnson,[1] J. T. Vaughey,[1] M. M. Thackeray[1]

[1] *Chemical Technology Division, Argonne National Laboratory, Argonne, IL, U.S.A.*
[2] *Chemistry Department, University of Florida, Gainesville, FL, U.S.A.*